INTERNATIONAL JOURNAL OF
NUMERICAL ANALYSIS AND MODELING
Volume 16, Number 5, Pages 695–717

NUMERICAL SOLUTION OF A TRANSIENT THREE-DIMENSIONAL EDDY CURRENT MODEL WITH MOVING CONDUCTORS

ALFREDO BERMÚDEZ, BIBIANA LÓPEZ-RODRÍGUEZ, RODOLFO RODRÍGUEZ,
AND PILAR SALGADO

Abstract. The aim of this paper is to propose and analyze a numerical method to solve a time-dependent eddy current problem in a domain containing moving non magnetic conductors. To this end, we choose a formulation in terms of the magnetic field, what leads to a parabolic problem for which we prove an existence result. For space discretization, we propose a finite element method based on Nédélec edge elements on a mesh that remains fixed over the time. The curl-free constraint in the dielectric domain is relaxed by means of a penalty strategy that can be easily implemented, without the need that the mesh fits the moving conducting and dielectric domains. For time discretization, we use a backward Euler scheme. We report some numerical results. First, we solve a test problem with a known analytical solution, which allows us to assess the convergence of the method as the penalization and discretization parameters go to zero. Finally, we solve a problem with cylindrical symmetry, which allows us to compare the results with those obtained with an axisymmetric code.

Key words. Eddy current problems, transient electromagnetic problems, moving domains, edge finite elements, penalty formulation.

1. Introduction

This paper deals with a finite element method to solve a time-dependent eddy current problem in a three-dimensional (3D) bounded domain containing moving non magnetic conductors. Such a problem arises in different physical applications such as electromagnetic forming process or magnetic levitation. In particular, our work is motivated by the simulation of electromagnetic forming processes (EMF) [8], which leads to solving the transient eddy current model with the conducting part being a workpiece which is deformed over the time due to electromagnetic forces, while the current source arises from a coil placed in a fixed position. A strategy often used in the literature to simulate this process is based on a sequential coupling [11] between an electromagnetic model and a structural one; the former allows computing the Lorentz-forces which drives the motion of the workpiece while the latter uses these forces as data to compute the workpiece deformation. In this way, the mechanical results would allow us to update the geometry to be used in the subsequent step of the electromagnetic model. To perform this coupling it is very useful to have an electromagnetic tool able to consider conducting subdomains whose form and position can change over the time. Thus, in this paper we develop a model for this purpose but we will assume that the geometry and position of the workpiece is known at any time. Our goal is to compute the eddy currents and thereby the Lorentz force in this moving conductor as a first step for a sequential magneto-mechanical coupling.

Received by the editors April 15, 2018.
2000 *Mathematics Subject Classification.* 65M60, 78M10.

The motion of the conductor introduces serious difficulties in the mathematical analysis of the eddy current model, mainly due to the different nature of the equations in the dielectric and conducting parts of the domain. In fact, to the best of our knowledge, there is no result guaranteeing the well-posedness of the 3D continuous problem.

Actually, there are just a few papers dealing with the analysis of the eddy current model considering moving conductors in either two or three dimensions. In particular, a two-dimensional transient eddy current problem arising from modeling electrical engines by considering the rotor motion has been analyzed in [5, 7]. The 3D case has been studied in [6], where a time-primitive of the electric field has been used as the main unknown leading to a degenerate parabolic problem. We notice that in these papers the interface between the moving and the fixed part is always the same. Moreover, the fact that the motion is a rotation is used in the theoretical proofs of existence and uniqueness of solution. Such a special kind of motion is quite different to what happens in other processes like EMF or magnetic levitation. From the point of view of the numerical solution, the techniques used in these papers are based on using different reference frames in the moving and non-moving parts, which involve Lagrangian formulations: this leads to work with independent meshes at each part of the domain, while the coupling transmission conditions are taken into account by using mortar techniques.

On the other hand, an axisymmetric eddy current model with workpiece motion has been more recently studied in [3, 4]. The main unknown in this case is a magnetic vector potential and the resulting problem is also parabolic and degenerate; the well-posedness of the problem is proved by means of a regularization argument. In this case, the problem is studied by using a unique reference frame. From the numerical point of view the proposal in these papers is to work with a fixed mesh over the whole time interval, even though the workpiece changes its position. This procedure is based on using low-order quadrature rules with a large number of integration points in those terms involving piecewise smooth discontinuous functions which appear due to the motion of the workpiece.

In this paper, we are interested in 3D problems where the conducting piece is not magnetic and moves freely in the dielectric domain and its motion is not necessarily rigid. From the mathematical point of view, to apply the above discussed results to this kind of problems does not seem to be feasible. In fact, the techniques from [6] do not seem to be applicable to these problems, because the geometry changes arbitrarily over the time. On the other hand, the approach from [3] is based on the fact that the cylindrical symmetry leads to a two-dimensional problem for a scalar variable and the proofs rely on a specific Reynold's transport theorem which does not hold in the present case.

Among the variety of possible formulations (see, for instance, [2]), for our choice we have prioritized three aspects: (i) the possibility of using a fixed mesh of the whole domain at all time, (ii) to avoid the need of building cutting surfaces (what can be extremely cumbersome in complex topologies) and (iii) to use a number of unknowns as small as possible. According to this, we have chosen a formulation in terms of the magnetic field which only involves this vector unknown in the whole domain. Let us remark that an alternative formulation with similar features could be based on a primitive of the electric field without using a gauge condition in the dielectric domain (see again [6]). The ideas used in the present paper regarding how to deal with a fixed mesh could be also tried in this case, although this choice would lead to solving a system with a singular matrix. Let us remark that we will not

neglect the velocity terms in Ohm's law in order to propose a general methodology to model physical applications in which this convective term may be relevant. Thus, the magnetic formulation leads to a parabolic problem with a convective term for which we obtain an existence result by following some ideas from [13]; however, uniqueness remains an open question.

Then, we introduce a numerical method to solve this problem based on Nédélec finite elements for space discretization combined with a backward Euler scheme for time discretization. The curl-free constraint in the dielectric domain is relaxed by means of a penalty strategy (see, for instance [10, Section I.4.3]). This approach applied to the eddy current model corresponds to replacing the dielectric domain by a so called *fake conductor*, namely, a material with a very low conductivity ([9]). Let us emphasize that in spite of the fact that the dielectric domain changes over the time, the proposed numerical method does not need moving meshes. Thus, to be able to use a fixed mesh, we resort to the same idea exploited in [4] in the axisymmetric case of using low-order quadrature rules with a large number of integration points for computing integrals involving discontinuous coefficients.

Although we do not have a convergence analysis for the numerical method applied to a problem with a moving workpiece, we report promissory numerical results obtained in a couple of test problems, which provide numerical evidence of the effectiveness of this approach. In particular, one of these tests is a problem on a cylindrical geometry, which allows us to compare our results with those obtained with the axisymmetric code from [4].

The outline of the paper is as follows. In Section 2, we introduce the time-dependent eddy current problem in a bounded domain with moving conductors and derive a weak formulation, for which we prove existence of solution. Then, we introduce two alternative formulations more adequate for numerical purposes; one of them is mixed while the other is a penalty formulation. The former can be seen as the limit of the latter as the penalization parameter goes to zero. We introduce numerical schemes to solve each of them and establish some advantages of the penalty formulation. In Section 3 we report numerical results for a couple of test problems. The first one is a problem with analytical solution that allows us to check the convergence properties of the proposed method. The second one is based on an axisymmetric setting and a rigid motion, and the results will be compared with those obtained in [4]. Finally, in Section 4, we draw some conclusions.

Throughout this paper, we will use classical Sobolev as well as other well-known spaces like $\mathrm{H}_0(\mathbf{curl};\omega) := \{\boldsymbol{G} \in \mathrm{H}(\mathbf{curl};\omega) : \boldsymbol{G} \times \boldsymbol{n} = \mathbf{0} \text{ on } \partial\omega\}$, $\mathrm{H}_0(\mathrm{div}^0;\omega) := \{\boldsymbol{F} \in \mathrm{H}(\mathrm{div};\omega) : \mathrm{div}\,\boldsymbol{F} = 0 \text{ in } \omega \text{ and } \boldsymbol{F}\cdot\boldsymbol{n} = 0 \text{ on } \partial\omega\}$, $\mathrm{H}_\gamma(\mathrm{div}^0;\omega) := \{\boldsymbol{F} \in \mathrm{H}(\mathrm{div};\omega) : \mathrm{div}\,\boldsymbol{F} = 0 \text{ in } \omega \text{ and } \boldsymbol{F}\cdot\boldsymbol{n} = 0 \text{ on } \gamma\}$, etc., for any subdomain $\omega \subseteq \Omega$ and any connected component γ of $\partial\omega$. Here and thereafter, we use boldface letters to denote vector fields and variables as well as vector-valued operators. Finally, C will denote strictly positive generic constants, not necessarily the same at each occurrence.

2. A magnetic field formulation on moving conductors

The aim of this section is to introduce a numerical method to solve transient eddy current problems on moving conductors with a fixed mesh. With this end, we propose a formulation based on the magnetic field. Then, we introduce a convenient weak form of this problem for which we prove existence of solution. Next, we propose a penalty method to deal with the curl-free constraint in the dielectric domain and we show that this penalized formulation has a unique solution, bounded

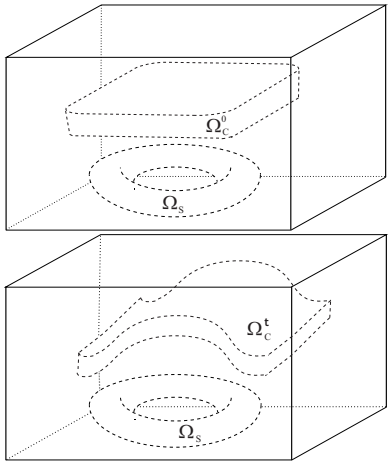

FIGURE 1. Sketch of the domain at initial time (up) and at time $t > 0$ (down).

independently of the penalization parameter. Finally we introduce a penalized fully discrete scheme which can be easily implemented on a fixed mesh that does not need to fit the conducting and dielectric domains.

2.1. Statement of the problem. Let us consider a coil which carries a given current density $\boldsymbol{J}_{\mathrm{S}}$ and a non-magnetic moving conducting workpiece. Let Ω be a simply connected bounded 3D domain with Lipschitz continuous connected boundary Γ, which contains the coil and the workpiece at all time t in an interval $[0,T]$. We assume that $\boldsymbol{J}_{\mathrm{S}}$ is supported in $\bar{\Omega}_{\mathrm{S}} \subset \Omega$. We are interested in computing the induced currents in the workpiece that moves over the time with a motion not necessarily rigid. Therefore, the domain occupied by the workpiece will depend on t and will be denoted by Ω_{C}^t. Obviously, its complement $\Omega_{\mathrm{D}}^t := \Omega \setminus \bar{\Omega}_{\mathrm{C}}^t$ also depends on t. We assume that Ω_{C}^t is connected and that $\bar{\Omega}_{\mathrm{C}}^t \cap \bar{\Omega}_{\mathrm{S}} = \emptyset$ for all $t \in [0,T]$ (see Figure 1). We notice that $\bar{\Omega}_{\mathrm{S}} \subset \Omega_{\mathrm{D}}^t$, so that $\boldsymbol{J}_{\mathrm{S}}|_{\Omega_{\mathrm{C}}^t} = \boldsymbol{0}$ at all time $t \in [0,T]$. We also notice that the domain Ω_{S} of the source current is assumed to be fixed over the whole time interval.

The problem to be solved is the following:

$$\partial_t(\mu \boldsymbol{H}) + \mathbf{curl}\, \boldsymbol{E} = \boldsymbol{0} \qquad \text{in } (0,T)\times\Omega, \tag{1}$$

$$\mathbf{curl}\, \boldsymbol{H} = \boldsymbol{J}_{\mathrm{S}} + \sigma \boldsymbol{E} + \sigma \boldsymbol{v} \times \mu \boldsymbol{H} \qquad \text{in } [0,T]\times\Omega, \tag{2}$$

$$\mathrm{div}(\mu \boldsymbol{H}) = 0 \qquad \text{in } [0,T]\times\Omega, \tag{3}$$

where $\boldsymbol{E}(t,\boldsymbol{x})$ is the electric field, $\boldsymbol{H}(t,\boldsymbol{x})$ the magnetic field, $\boldsymbol{v}(t,\boldsymbol{x})$ the velocity at each point $\boldsymbol{x}$ of the workpiece, μ the magnetic permeability and $\sigma(t,\boldsymbol{x})$ the electric conductivity.

We assume that the source current $\boldsymbol{J}_{\mathrm{S}}|_{\Omega_{\mathrm{S}}} \in \mathrm{H}^1(0,T;\mathrm{H}_0(\mathrm{div}^0;\Omega_{\mathrm{S}}))$. Moreover, since $\boldsymbol{J}_{\mathrm{S}}$ is supported in $\bar{\Omega}_{\mathrm{S}}$, this implies that its extension by zero belongs to $\mathrm{H}^1(0,T;\mathrm{H}_0(\mathrm{div}^0;\Omega))$, too. On the other hand, since the workpiece is assumed to be non magnetic, the permeability is constant in the whole domain Ω: $\mu = \mu_0$, with μ_0 being the magnetic permeability of vacuum. In turn, σ vanishes in the dielectric and varies with time and space in the conductors; moreover, we assume that there

exist positive constants $\underline{\sigma}$ and $\overline{\sigma}$, lower and upper bounds of σ, respectively; namely,

$$0 < \underline{\sigma} \le \sigma(t, \boldsymbol{x}) \le \overline{\sigma}, \quad \boldsymbol{x} \in \Omega_{\mathrm{C}}^t \qquad \text{and} \qquad \sigma \equiv 0 \text{ in } \Omega_{\mathrm{D}}^t, \quad t \in [0, T].$$

Finally, each point of the workpiece is assumed to move with a given bounded velocity $\boldsymbol{v}$ which satisfies

$$|\boldsymbol{v}(t, \boldsymbol{x})| \le \|\boldsymbol{v}\|_\infty < \infty, \qquad \boldsymbol{x} \in \Omega_{\mathrm{C}}^t, \quad t \in [0, T].$$

Equations (1)–(3) must be completed with suitable boundary and initial conditions. For the latter, we consider

$$\boldsymbol{H}(0, \boldsymbol{x}) = \boldsymbol{H}_0(\boldsymbol{x}) \qquad \boldsymbol{x} \in \Omega, \tag{4}$$

where $\boldsymbol{H}_0 \in \mathrm{H}_0(\mathbf{curl}; \Omega)$ and satisfies $\operatorname{div}(\mu \boldsymbol{H}_0) = 0$ in Ω. Note that this last equation together with (1) imply that $\boldsymbol{H}$ satisfies (3) at all time $t \in [0, T]$.

The transient eddy current model (1)–(4) defined in the whole space $\mathbb{R}^3$ with appropriate conditions at infinity and fixed conductors has been studied in [12]. In our case, we restrict our analysis to a bounded domain Ω and consider the following homogeneous boundary conditions:

$$\boldsymbol{H} \times \boldsymbol{n} = \boldsymbol{0} \qquad \text{on } [0, T] \times \Gamma. \tag{5}$$

Let us remark that this is a reasonable approximation, provided the domain Ω is chosen sufficiently large so that its boundary is far enough from Ω_{S} and Ω_{C}^t for all $t \in [0, T]$.

To obtain a weak formulation of this problem for which the existence of a solution will be established, we use an auxiliary vector field $\widehat{\boldsymbol{H}} \in \mathrm{H}^1(0, T; \mathrm{H}_0(\mathbf{curl}; \Omega))$ satisfying $\mathbf{curl}\, \widehat{\boldsymbol{H}} = \boldsymbol{J}_{\mathrm{S}}$ in Ω. In order to define such an $\widehat{\boldsymbol{H}}$, we use that, since $\partial_t \boldsymbol{J}_{\mathrm{S}}(t) \in \mathrm{H}_0(\operatorname{div}^0; \Omega)$ and Ω is simply connected, there exists a unique vector potential $\boldsymbol{Q}(t) \in \mathrm{H}_0(\mathbf{curl}; \Omega)$ such that

$$\mathbf{curl}\, \boldsymbol{Q}(t) = \partial_t \boldsymbol{J}_{\mathrm{S}}(t) \qquad \text{in } \Omega \tag{6}$$

and $\operatorname{div} \boldsymbol{Q}(t) = 0$ in Ω (see [10, Theorem I.3.6]). Moreover, there exists $C > 0$ such that $\|\boldsymbol{Q}(t)\|_{\mathrm{H}(\mathbf{curl};\Omega)} \le C \|\partial_t \boldsymbol{J}_{\mathrm{S}}(t)\|_{\mathrm{L}^2(\Omega_{\mathrm{S}})^3}$. Then,

$$\int_0^T \|\boldsymbol{Q}(t)\|^2_{\mathrm{H}(\mathbf{curl};\Omega)}\, dt \le C \int_0^T \|\partial_t \boldsymbol{J}_{\mathrm{S}}(t)\|^2_{\mathrm{L}^2(\Omega_{\mathrm{S}})^3}\, dt \le C \|\boldsymbol{J}_{\mathrm{S}}\|^2_{\mathrm{H}^1(0,T;\mathrm{L}^2(\Omega_{\mathrm{S}})^3)} < \infty. \tag{7}$$

Similarly, since $\boldsymbol{J}_{\mathrm{S}}(0) \in \mathrm{H}_0(\operatorname{div}^0; \Omega)$ as well, there also exists a unique vector potential $\boldsymbol{R}_0 \in \mathrm{H}_0(\mathbf{curl}; \Omega)$ such that

$$\mathbf{curl}\, \boldsymbol{R}_0 = \boldsymbol{J}_{\mathrm{S}}(0) \qquad \text{in } \Omega, \tag{8}$$

$\operatorname{div} \boldsymbol{R}_0 = 0$ in Ω and $\|\boldsymbol{R}_0\|_{\mathrm{H}(\mathbf{curl};\Omega)} \le C \|\boldsymbol{J}_{\mathrm{S}}(0)\|_{\mathrm{L}^2(\Omega_{\mathrm{S}})^3}$. Therefore, we define

$$\widehat{\boldsymbol{H}}(t) := \boldsymbol{R}_0 + \int_0^t \boldsymbol{Q}(s)\, ds, \tag{9}$$

so that $\partial_t \widehat{\boldsymbol{H}}(t) = \boldsymbol{Q}(t)$ in the sense of distributions in $(0, T)$ (see [16, Remark 131(b)], for instance). Then, from (7) we have

$$\int_0^T \left\|\partial_t \widehat{\boldsymbol{H}}(t)\right\|^2_{\mathrm{H}(\mathbf{curl};\Omega)} dt = \int_0^T \|\boldsymbol{Q}(t)\|^2_{\mathrm{H}(\mathbf{curl};\Omega)}\, dt < \infty.$$

On the other hand, straightforward computations allow us to bound $\int_0^T \left\|\widehat{\boldsymbol{H}}(t)\right\|^2_{\mathrm{H}(\mathbf{curl};\Omega)} dt$ too, so that we conclude that $\widehat{\boldsymbol{H}} \in \mathrm{H}^1(0, T; \mathrm{H}_0(\mathbf{curl}; \Omega))$ and

$$\left\|\widehat{\boldsymbol{H}}\right\|_{\mathrm{H}^1(0,T;\mathrm{H}(\mathbf{curl};\Omega))} \le C \|\boldsymbol{J}_{\mathrm{S}}\|_{\mathrm{H}^1(0,T;\mathrm{L}^2(\Omega_{\mathrm{S}})^3)}. \tag{10}$$

Furthermore, from (9), (8), (6) and [16, Theorems 111 & 127] we have that

$$\mathbf{curl}\,\widehat{\boldsymbol{H}}(t) = \mathbf{curl}\,\boldsymbol{R}_0 + \int_0^t \mathbf{curl}\,\boldsymbol{Q}(s)\,ds = \boldsymbol{J}_{\mathrm{S}}(t) \qquad \text{in } \Omega, \quad t \in [0,T].$$

Now, we write $\boldsymbol{H} = \widetilde{\boldsymbol{H}} + \widehat{\boldsymbol{H}}$, so that equations (1)–(5) lead to

$$\partial_t(\mu\widetilde{\boldsymbol{H}}) + \mathbf{curl}\,\boldsymbol{E} = -\partial_t(\mu\widehat{\boldsymbol{H}}) \qquad \text{in } [0,T]\times\Omega, \tag{11}$$

$$\mathbf{curl}\,\widetilde{\boldsymbol{H}} - \sigma\,\boldsymbol{v}\times\mu\widetilde{\boldsymbol{H}} = \sigma\boldsymbol{E} + \sigma\,\boldsymbol{v}\times\mu\widehat{\boldsymbol{H}} \qquad \text{in } [0,T]\times\Omega, \tag{12}$$

$$\widetilde{\boldsymbol{H}}\times\boldsymbol{n} = \boldsymbol{0} \qquad \text{on } [0,T]\times\Gamma, \tag{13}$$

$$\widetilde{\boldsymbol{H}}(0) = \boldsymbol{H}_0 - \widehat{\boldsymbol{H}}(0) \qquad \text{in } \Omega. \tag{14}$$

For each $t\in[0,T]$, we define

$$\boldsymbol{\mathcal{Y}}_t := \left\{\boldsymbol{G}\in \mathrm{H}_0(\mathbf{curl};\Omega):\ \mathbf{curl}\,\boldsymbol{G} = \boldsymbol{0} \text{ in } \Omega_{\mathrm{D}}^t\right\},$$
$$\mathrm{L}^2(0,T;\boldsymbol{\mathcal{Y}}_t) := \left\{\boldsymbol{G}\in \mathrm{L}^2(0,T;\mathrm{H}_0(\mathbf{curl};\Omega)):\ \boldsymbol{G}(t)\in\boldsymbol{\mathcal{Y}}_t,\ t\in[0,T]\right\}.$$

The latter is a closed subspace of $\mathrm{L}^2(0,T;\mathrm{H}_0(\mathbf{curl};\Omega))$ and hence a Hilbert space (cf. [13]).

Notice that, because of (12) and the fact that σ vanishes in Ω_{D}^t, we have that $\widetilde{\boldsymbol{H}}\in\mathrm{L}^2(0,T;\boldsymbol{\mathcal{Y}}_t)$. By testing (11) with $\boldsymbol{G}\in\mathrm{L}^2(0,T;\boldsymbol{\mathcal{Y}}_t)$ and integrating by parts, we write

$$\int_\Omega \partial_t(\mu\widetilde{\boldsymbol{H}})\cdot\boldsymbol{G} + \int_{\Omega_{\mathrm{C}}^t}\boldsymbol{E}\cdot\mathbf{curl}\,\boldsymbol{G} = -\int_\Omega \partial_t(\mu\widehat{\boldsymbol{H}})\cdot\boldsymbol{G}.$$

Hence, using (12) to eliminate $\boldsymbol{E}$ we obtain

$$\int_\Omega \partial_t(\mu\widetilde{\boldsymbol{H}})\cdot\boldsymbol{G} + \int_{\Omega_{\mathrm{C}}^t}\frac{1}{\sigma}\,\mathbf{curl}\,\widetilde{\boldsymbol{H}}\cdot\mathbf{curl}\,\boldsymbol{G} - \int_{\Omega_{\mathrm{C}}^t}\boldsymbol{v}\times\mu\widetilde{\boldsymbol{H}}\cdot\mathbf{curl}\,\boldsymbol{G} = -\int_\Omega \partial_t(\mu\widehat{\boldsymbol{H}})\cdot\boldsymbol{G} + \int_{\Omega_{\mathrm{C}}^t}\boldsymbol{v}\times\mu\widehat{\boldsymbol{H}}\cdot\mathbf{curl}\,\boldsymbol{G}. \tag{15}$$

Let $f\in\mathrm{L}^2(0,T;\mathrm{H}_0(\mathbf{curl};\Omega)')$ be defined by

$$\langle f(t),\boldsymbol{G}\rangle := -\int_\Omega \partial_t(\mu\widehat{\boldsymbol{H}}(t))\cdot\boldsymbol{G} + \int_{\Omega_{\mathrm{C}}^t}\boldsymbol{v}\times\mu\widehat{\boldsymbol{H}}(t)\cdot\mathbf{curl}\,\boldsymbol{G} \qquad \forall\boldsymbol{G}\in\mathrm{H}_0(\mathbf{curl};\Omega),$$

where $\langle\cdot,\cdot\rangle$ denotes the duality pairing between $\mathrm{H}_0(\mathbf{curl};\Omega)$ and $\mathrm{H}_0(\mathbf{curl};\Omega)'$. Let $a(t;\cdot,\cdot)$ be the continuous bilinear form defined in $\mathrm{H}_0(\mathbf{curl};\Omega)\times\mathrm{H}_0(\mathbf{curl};\Omega)$ by

$$a(t;\widetilde{\boldsymbol{G}},\boldsymbol{G}) := \int_{\Omega_{\mathrm{C}}^t}\frac{1}{\sigma(t)}\,\mathbf{curl}\,\widetilde{\boldsymbol{G}}\cdot\mathbf{curl}\,\boldsymbol{G} - \int_{\Omega_{\mathrm{C}}^t}\boldsymbol{v}(t)\times\mu\widetilde{\boldsymbol{G}}\cdot\mathbf{curl}\,\boldsymbol{G}$$

and $c(\cdot,\cdot)$ the continuous bilinear form defined in $\mathrm{L}^2(\Omega)^3\times\mathrm{L}^2(\Omega)^3$ by

$$c(\widetilde{\boldsymbol{G}},\boldsymbol{G}) := \int_\Omega \mu\,\widetilde{\boldsymbol{G}}\cdot\boldsymbol{G}.$$

Then, integrating by parts in time the first term in (15) leads us to the following weak form of problem (1)–(5):

Problem 1. *Find* $\widetilde{\boldsymbol{H}}\in\mathrm{L}^2(0,T;\boldsymbol{\mathcal{Y}}_t)$ *such that*

$$\int_0^T a(t;\widetilde{\boldsymbol{H}}(t),\boldsymbol{G}(t))\,dt - \int_0^T c(\widetilde{\boldsymbol{H}}(t),\partial_t\boldsymbol{G}(t))\,dt = \int_0^T\langle f(t),\boldsymbol{G}(t)\rangle\,dt + c(\boldsymbol{H}_0-\widehat{\boldsymbol{H}}(0),\boldsymbol{G}(0))$$

for all $\boldsymbol{G} \in \mathrm{L}^2(0,T;\boldsymbol{\mathcal{Y}}_t) \cap \mathrm{H}^1(0,T;\mathrm{L}^2(\Omega)^3)$ *with* $\boldsymbol{G}(T) = \mathbf{0}$ *in* Ω.

Now, we are in a position to apply results from [13] to prove the existence of solution to this problem.

Theorem 1. *Problem 1 has a solution.*

Proof. The result is an application of Theorem 1 from [13]. In fact, since μ is assumed to be time-independent, the bilinear form $c(\cdot,\cdot)$ does not depend on t and hence we only need to check the following hypotheses of this theorem:

(i) $\boldsymbol{\mathcal{Y}}_t \subset \mathrm{H}_0(\mathbf{curl};\Omega) \subset \mathrm{L}^2(\Omega)^3$;
(ii) $c(\boldsymbol{G},\boldsymbol{G}) \geq 0 \quad \forall \boldsymbol{G} \in \mathrm{L}^2(\Omega)^3$;
(iii) $\exists \lambda, \alpha > 0 : \quad \lambda\, c(\boldsymbol{G},\boldsymbol{G}) + a(t;\boldsymbol{G},\boldsymbol{G}) \geq \alpha \left\|\boldsymbol{G}\right\|^2_{\mathrm{H}(\mathbf{curl};\Omega)} \quad \forall \boldsymbol{G} \in \boldsymbol{\mathcal{Y}}_t, \quad$ a.e. $t \in [0,T]$.

Properties (i) and (ii) clearly hold in our case. The last property is a Gårding inequality that holds true for any sufficiently large λ. In fact, using Young's inequality, we have that

$$\left| \int_{\Omega_{\mathrm{C}}^t} \boldsymbol{v}(t) \times \mu \boldsymbol{G} \cdot \mathbf{curl}\, \boldsymbol{G} \right| \leq \mu \left\|\boldsymbol{v}\right\|_\infty \left\{ \frac{\gamma}{2} \left\|\boldsymbol{G}\right\|^2_{\mathrm{L}^2(\Omega)^3} + \frac{1}{2\gamma} \left\|\mathbf{curl}\, \boldsymbol{G}\right\|^2_{\mathrm{L}^2(\Omega_{\mathrm{C}}^t)^3} \right\}$$

for all $\gamma > 0$ and, consequently,

$$\begin{aligned} (16) \qquad & \lambda\, c(\boldsymbol{G},\boldsymbol{G}) + a(t;\boldsymbol{G},\boldsymbol{G}) \\ & \geq \left(\lambda\mu - \frac{\gamma}{2}\mu \left\|\boldsymbol{v}\right\|_\infty\right) \left\|\boldsymbol{G}\right\|^2_{\mathrm{L}^2(\Omega)^3} + \left(\frac{1}{\overline{\sigma}} - \frac{1}{2\gamma}\mu \left\|\boldsymbol{v}\right\|_\infty\right) \left\|\mathbf{curl}\, \boldsymbol{G}\right\|^2_{\mathrm{L}^2(\Omega_{\mathrm{C}}^t)^3}. \end{aligned}$$

Hence, by taking $\gamma = \overline{\sigma}\mu \left\|\boldsymbol{v}\right\|_\infty$, we write

$$\begin{aligned} & \lambda\, c(\boldsymbol{G},\boldsymbol{G}) + a(t;\boldsymbol{G},\boldsymbol{G}) \\ & \geq \min\left\{ \lambda\mu - \frac{1}{2}\overline{\sigma}\mu^2 \left\|\boldsymbol{v}\right\|^2_\infty, \frac{1}{2\overline{\sigma}} \right\} \left\|\boldsymbol{G}\right\|^2_{\mathrm{H}(\mathbf{curl};\Omega)} \qquad \forall \boldsymbol{G} \in \boldsymbol{\mathcal{Y}}_t, \quad t \in [0,T]. \end{aligned}$$

Therefore, property (iii) holds true for any $\lambda > \frac{\overline{\sigma}\mu\|\boldsymbol{v}\|^2_\infty}{2}$ with $\alpha = \min\left\{ \lambda\mu - \frac{1}{2}\overline{\sigma}\mu^2 \left\|\boldsymbol{v}\right\|^2_\infty, \frac{1}{2\overline{\sigma}} \right\} > 0$. Thus, we conclude the proof. □

Unfortunately, we cannot apply Theorem 2 from [13] to conclude that Problem 1 has a unique solution, because two of the hypotheses of this theorem are not fulfilled in this case. On one side, the set $\{a(t;\cdot,\cdot) : t \in [0,T]\}$ should be a regular family on $\boldsymbol{\mathcal{Y}}_t$. For this property to hold, apparently we would need a Reynold's transport formula for $|\mathbf{curl}\, \boldsymbol{G}|^2$ with $\boldsymbol{G} \in \boldsymbol{\mathcal{Y}}_t \subset \mathrm{H}_0(\mathbf{curl};\Omega)$. Recently, a version of such a formula for functions with reduced smoothness was proved in [3], however it seems mandatory that the integrand (in our case $|\mathbf{curl}\, \boldsymbol{G}|^2$) be in $\mathrm{W}^{1,1}(\Omega)$, which is not the case in the problem we are dealing with. On the other hand, another hypothesis of Theorem 2 from [13] is that the family of spaces $\boldsymbol{\mathcal{Y}}_t$ has to be decreasing in the sense that

$$\forall\, t, s \in [0,T] \quad t > s \Rightarrow \boldsymbol{\mathcal{Y}}_t \subset \boldsymbol{\mathcal{Y}}_s.$$

This would hold in our case only if the workpiece shrinks without other motion, which would be a rather particular case. Thus, the uniqueness of the solution to Problem 1 remains an open question.

2.2. Mixed and penalty formulations. The formulation in Problem 1 is useful to prove the existence of solution to (1)–(5), but not for computational purposes. In order to numerically solve this problem, we introduce in this subsection two more convenient alternative formulations. The former is a mixed one, in which the constraint

$$\mathbf{curl}\,\boldsymbol{H}(t) = \boldsymbol{J}_{\mathrm{S}}(t) \qquad \text{in } \Omega_{\mathrm{D}}^t \tag{17}$$

that follows from (2) is imposed by means of a Lagrange multiplier. The second one is based on relaxing this constraint by means of a penalization technique.

To derive a mixed formulation of problem (1)–(5), we integrate (1) multiplied by a time-independent test function $\boldsymbol{G} \in \mathrm{H}_0(\mathbf{curl};\Omega)$, integrate by parts and use (2) to substitute $\boldsymbol{E}$ in terms of $\mathbf{curl}\,\boldsymbol{H}$ and $\boldsymbol{v}\times\mu\boldsymbol{H}$ in Ω_{C}^t. The resulting equation combined with a weak form of constraint (17) lead us to the following.

Problem 2. *Find* $\boldsymbol{H} \in \mathrm{L}^2(0,T;\mathrm{H}_0(\mathbf{curl};\Omega)) \cap \mathrm{H}^1(0,T;\mathrm{H}_0(\mathbf{curl};\Omega)')$ *and* $\boldsymbol{E} \in \mathrm{L}^2(0,T;\mathrm{H}_\Gamma(\mathrm{div}^0;\Omega_{\mathrm{D}}^t))$ *such that*

$$\begin{aligned}
&\frac{d}{dt}\int_\Omega \mu\boldsymbol{H}\cdot\boldsymbol{G} + \int_{\Omega_{\mathrm{C}}^t}\frac{1}{\sigma}\,\mathbf{curl}\,\boldsymbol{H}\cdot\mathbf{curl}\,\boldsymbol{G}\\
&-\int_{\Omega_{\mathrm{C}}^t}\boldsymbol{v}\times\mu\boldsymbol{H}\cdot\mathbf{curl}\,\boldsymbol{G} + \int_{\Omega_{\mathrm{D}}^t}\mathbf{curl}\,\boldsymbol{G}\cdot\boldsymbol{E} = 0 \qquad \forall\boldsymbol{G}\in\mathrm{H}_0(\mathbf{curl};\Omega),\\
&\int_{\Omega_{\mathrm{D}}^t}\mathbf{curl}\,\boldsymbol{H}\cdot\boldsymbol{F} = \int_{\Omega_{\mathrm{S}}}\boldsymbol{J}_{\mathrm{S}}\cdot\boldsymbol{F} \qquad \forall\boldsymbol{F}\in\mathrm{H}_\Gamma(\mathrm{div}^0;\Omega_{\mathrm{D}}^t),\\
&\boldsymbol{H}(0) = \boldsymbol{H}_0 \qquad \textit{in } \Omega.
\end{aligned}$$

This mixed formulation has been introduced and analyzed in the case of fixed conductors in [1] and [12], in the harmonic and the time-domain regimes, respectively. However, when the dielectric domain changes over the time, the mathematical analysis of this problem does not follow from the same arguments used in these references.

On the other hand, the finite element approximation of this mixed problem looks expensive, since two vector fields have to be discretized: $\boldsymbol{H}$ in the whole domain and $\boldsymbol{E}$ in the dielectric (which moves over the time). Moreover, as it will be explained in more detail in the following subsection, it is not immediate to find a basis of the finite element space used to discretize the space $\mathrm{H}_\Gamma(\mathrm{div}^0;\Omega_{\mathrm{D}}^t)$ where the Lagrange multiplier lies.

Instead of pursuing this approach, we resort to a penalization technique to relax constraint (17). The penalization consists in assuming that the dielectric is not a perfect insulator but a fake conductor; namely, a material with a very low conductivity $\varepsilon > 0$. More precisely, instead of (17) we impose

$$\mathbf{curl}\,\boldsymbol{H}(t) - \boldsymbol{J}_{\mathrm{S}}(t) = \varepsilon\boldsymbol{E}(t) \qquad \text{in } \Omega_{\mathrm{D}}^t,$$

where ε is a small positive parameter. For the forthcoming analysis, we will consider $\varepsilon \in (0,\underline{\sigma})$, which is not restrictive at all since, in practice, ε is taken significantly smaller than $\underline{\sigma}$. Therefore, for any such ε, the same steps that lead to Problem 2, but using now the above equation to substitute $\boldsymbol{E}$ in terms of $\boldsymbol{H}$ and $\boldsymbol{J}_{\mathrm{S}}$ in Ω_{D}^t, yield the following penalized form of problem (1)–(5).

Problem 3. *Find* $\boldsymbol{H}_\varepsilon \in \mathrm{L}^2(0,T;\mathrm{H}_0(\mathbf{curl};\Omega)) \cap \mathrm{H}^1(0,T;\mathrm{H}_0(\mathbf{curl};\Omega)')$ *such that*

$$\frac{d}{dt}\int_\Omega \mu \boldsymbol{H}_\varepsilon \cdot \boldsymbol{G} + \int_{\Omega_{\mathrm{C}}^t} \frac{1}{\sigma}\,\mathbf{curl}\,\boldsymbol{H}_\varepsilon \cdot \mathbf{curl}\,\boldsymbol{G} - \int_{\Omega_{\mathrm{C}}^t} \boldsymbol{v}\times\mu\boldsymbol{H}_\varepsilon \cdot \mathbf{curl}\,\boldsymbol{G} + \frac{1}{\varepsilon}\int_{\Omega_{\mathrm{D}}^t} \mathbf{curl}\,\boldsymbol{H}_\varepsilon \cdot \mathbf{curl}\,\boldsymbol{G} = \frac{1}{\varepsilon}\int_{\Omega_{\mathrm{S}}} \boldsymbol{J}_{\mathrm{S}} \cdot \mathbf{curl}\,\boldsymbol{G} \qquad \forall \boldsymbol{G} \in \mathrm{H}_0(\mathbf{curl};\Omega),$$

$$\boldsymbol{H}_\varepsilon(0) = \boldsymbol{H}_0 \qquad \text{in } \Omega.$$

The above problem is well posed and its solution is bounded uniformly in ε as it is shown in what follows.

Proposition 1. *For any* $\varepsilon \in (0,\underline{\sigma})$*, Problem 3 has a unique solution* $\boldsymbol{H}_\varepsilon$*. Moreover, there exists a constant* $C>0$*, independent of* ε*,* $\boldsymbol{J}_{\mathrm{S}}$ *and* $\boldsymbol{H}_0$*, such that*

$$\|\boldsymbol{H}_\varepsilon\|^2_{\mathrm{L}^\infty(0,T;\mathrm{L}^2(\Omega)^3)} + \|\mathbf{curl}\,\boldsymbol{H}_\varepsilon\|^2_{\mathrm{L}^2(0,T;\mathrm{L}^2(\Omega)^3)} \le C\left\{\|\boldsymbol{H}_0\|^2_{\mathrm{L}^2(\Omega)^3} + \|\boldsymbol{J}_{\mathrm{S}}\|^2_{\mathrm{H}^1(0,T;\mathrm{L}^2(\Omega_{\mathrm{S}})^3)}\right\}.$$

Proof. First, we proceed as we did to derive (15). In fact, let $\widehat{\boldsymbol{H}}$ be defined by (9) and let $\widetilde{\boldsymbol{H}}_\varepsilon$ be such that $\boldsymbol{H}_\varepsilon = \widetilde{\boldsymbol{H}}_\varepsilon + \widehat{\boldsymbol{H}}$. Substituting this into Problem 3 we obtain

$$\begin{aligned}(18)\qquad &\frac{d}{dt}\int_\Omega \mu\widetilde{\boldsymbol{H}}_\varepsilon \cdot \boldsymbol{G} + \int_{\Omega_{\mathrm{C}}^t} \frac{1}{\sigma}\,\mathbf{curl}\,\widetilde{\boldsymbol{H}}_\varepsilon \cdot \mathbf{curl}\,\boldsymbol{G}\\ &- \int_{\Omega_{\mathrm{C}}^t} \boldsymbol{v}\times\mu\widetilde{\boldsymbol{H}}_\varepsilon \cdot \mathbf{curl}\,\boldsymbol{G} + \frac{1}{\varepsilon}\int_{\Omega_{\mathrm{D}}^t} \mathbf{curl}\,\widetilde{\boldsymbol{H}}_\varepsilon \cdot \mathbf{curl}\,\boldsymbol{G}\\ &= -\int_\Omega \partial_t(\mu\widehat{\boldsymbol{H}})\cdot\boldsymbol{G} + \int_{\Omega_{\mathrm{C}}^t} \boldsymbol{v}\times\mu\widehat{\boldsymbol{H}}\cdot\mathbf{curl}\,\boldsymbol{G} \qquad \forall \boldsymbol{G}\in\mathrm{H}_0(\mathbf{curl};\Omega),\end{aligned}$$

$$(19)\qquad \widetilde{\boldsymbol{H}}_\varepsilon(0) = \boldsymbol{H}_0 - \widehat{\boldsymbol{H}}(0) \qquad \text{in } \Omega.$$

The existence of a unique solution $\widetilde{\boldsymbol{H}}_\varepsilon$ of the above problem is a consequence of [14, Proposition III.2.3]. Indeed, the continuous bilinear form defined in $\mathrm{H}_0(\mathbf{curl};\Omega)\times\mathrm{H}_0(\mathbf{curl};\Omega)$ by

$$a_\varepsilon(t;\widetilde{\boldsymbol{G}},\boldsymbol{G}) := \int_{\Omega_{\mathrm{C}}^t} \frac{1}{\sigma(t)}\,\mathbf{curl}\,\widetilde{\boldsymbol{G}}\cdot\mathbf{curl}\,\boldsymbol{G} + \int_{\Omega_{\mathrm{D}}^t} \frac{1}{\varepsilon}\,\mathbf{curl}\,\widetilde{\boldsymbol{G}}\cdot\mathbf{curl}\,\boldsymbol{G} - \int_{\Omega_{\mathrm{C}}^t} \boldsymbol{v}(t)\times\mu\widetilde{\boldsymbol{G}}\cdot\mathbf{curl}\,\boldsymbol{G}$$

satisfies

$$a_\varepsilon(t;\boldsymbol{G},\boldsymbol{G}) = a(t;\boldsymbol{G},\boldsymbol{G}) + \int_{\Omega_{\mathrm{D}}^t} \frac{1}{\varepsilon}|\,\mathbf{curl}\,\boldsymbol{G}|^2.$$

Hence $a_\varepsilon(t;\cdot,\cdot)$ satisfies a Gårding inequality in $\mathrm{H}(\mathbf{curl};\Omega)$ with the same parameters λ and α as in the proof of Theorem 1. This property combined with an exponential shift allow us to use [14, Proposition III.2.3] to prove the existence of a unique solution of (18)–(19).

Now, for the *a priori* estimate, we take $\boldsymbol{G} = \widetilde{\boldsymbol{H}}_\varepsilon(t)$ in (18) and apply standard arguments (Young's inequality, Gronwall's lemma and time integration) to derive that, for $\varepsilon < \underline{\sigma}$, there exists $C>0$ independent of ε such that

$$\begin{aligned}\|\widetilde{\boldsymbol{H}}_\varepsilon\|^2_{\mathrm{L}^\infty(0,T;\mathrm{L}^2(\Omega)^3)} + \|\,\mathbf{curl}\,\widetilde{\boldsymbol{H}}_\varepsilon\|^2_{\mathrm{L}^2(0,T;\mathrm{L}^2(\Omega)^3)}&\\ \le C\left\{\|\widetilde{\boldsymbol{H}}_\varepsilon(0)\|^2_{\mathrm{L}^2(\Omega)^3} + \|\widehat{\boldsymbol{H}}\|^2_{\mathrm{H}^1(0,T;\mathrm{L}^2(\Omega)^3)}\right\}&\\ \le C\left\{\|\boldsymbol{H}_0\|^2_{\mathrm{L}^2(\Omega)^3} + \|\boldsymbol{J}_{\mathrm{S}}\|^2_{\mathrm{H}^1(0,T;\mathrm{L}^2(\Omega_{\mathrm{S}})^3)}\right\},&\end{aligned}$$

where we have used (10) for the last inequality. □

2.3. Discretization. The aim of this subsection is to introduce a numerical method to approximate the solution of Problem 3. Before doing this, we will present a discretization of Problem 2, which can be seen as the limit case of Problem 3 as ε goes to zero. The reason for this is two-fold. On one side, it will allow us to make it clear that solving Problem 3 is less expensive than solving Problem 2. On the other hand, in the next section, we will use the numerical solution of Problem 2 to estimate the dependence of the error on the parameter ε and thus to establish how small must be chosen ε in practice.

From now on, we assume that Ω and Ω_{S} are Lipschitz polyhedra and consider a regular family of tetrahedral meshes $\mathcal{T}_h$ of Ω, such that each element $K \in \mathcal{T}_h$ is contained either in $\bar{\Omega}_{\mathrm{S}}$ or in $\bar{\Omega} \setminus \Omega_{\mathrm{S}}$ (h stands, as usual, for the corresponding mesh-size). We employ edge finite elements to approximate the magnetic field; more precisely, elements from the lowest-order Nédélec space

$$\boldsymbol{\mathcal{N}}_h(\Omega) := \{\boldsymbol{G}_h \in \mathrm{H}(\mathbf{curl};\Omega) :\ \boldsymbol{G}_h|_K \in \boldsymbol{\mathcal{N}}(K)\ \ \forall K \in \mathcal{T}_h\},$$

where

$$\boldsymbol{\mathcal{N}}(K) := \left\{\boldsymbol{G}_h \in \mathbb{P}_1^3 :\ \boldsymbol{G}_h(\boldsymbol{x}) = \boldsymbol{a} \times \boldsymbol{x} + \boldsymbol{b},\ \boldsymbol{a}, \boldsymbol{b} \in \mathbb{R}^3,\ \boldsymbol{x} \in K\right\}.$$

We introduce the discrete subspace

$$\boldsymbol{\mathcal{N}}_h^{\Gamma}(\Omega) = \{\boldsymbol{G}_h \in \boldsymbol{\mathcal{N}}_h(\Omega) :\ \boldsymbol{G}_h \times \boldsymbol{n} = \boldsymbol{0} \text{ on } \Gamma\} \subset \mathrm{H}_0(\mathbf{curl};\Omega).$$

To discretize in time Problem 2, we use a backward Euler scheme on a uniform partition of $[0,T]$: $t_m := m\Delta t$, $m = 0, \ldots, M$, with time-step $\Delta t := \frac{T}{M}$. Finally, we use an approximate initial data $\boldsymbol{H}_{0h} \in \boldsymbol{\mathcal{N}}_h^{\Gamma}(\Omega)$ (for instance, the Nédélec interpolant of $\boldsymbol{H}_0$, provided this initial data is smooth enough for this interpolant to be well defined). Thus we are led to the following problem, where

$$\boldsymbol{\mathcal{N}}_h^{\Gamma}(\Omega_{\mathrm{D}}^{t_m}) := \left\{\boldsymbol{G}_h|_{\Omega_{\mathrm{D}}^{t_m}} :\ \boldsymbol{G}_h \in \boldsymbol{\mathcal{N}}_h^{\Gamma}(\Omega)\right\}, \qquad m = 0, \ldots, M.$$

Problem 4. *Let $\boldsymbol{H}_h^0 := \boldsymbol{H}_{0h}$. For $m = 1, \ldots, M$, find $\boldsymbol{H}_h^m \in \boldsymbol{\mathcal{N}}_h^{\Gamma}(\Omega)$ and $\boldsymbol{E}_h^m \in \mathbf{curl}\left(\boldsymbol{\mathcal{N}}_h^{\Gamma}(\Omega_{\mathrm{D}}^{t_m})\right)$ such that*

$$\int_{\Omega} \mu\, \frac{\boldsymbol{H}_h^m - \boldsymbol{H}_h^{m-1}}{\Delta t} \cdot \boldsymbol{G}_h + \int_{\Omega_{\mathrm{C}}^{t_m}} \frac{1}{\sigma}\, \mathbf{curl}\, \boldsymbol{H}_h^m \cdot \mathbf{curl}\, \boldsymbol{G}_h - \int_{\Omega_{\mathrm{C}}^{t_m}} \boldsymbol{v} \times \mu \boldsymbol{H}_h^m \cdot \mathbf{curl}\, \boldsymbol{G}_h$$
$$+ \int_{\Omega_{\mathrm{D}}^{t_m}} \mathbf{curl}\, \boldsymbol{G}_h \cdot \boldsymbol{E}_h^m = 0 \quad \forall \boldsymbol{G}_h \in \boldsymbol{\mathcal{N}}_h^{\Gamma}(\Omega),$$
$$\int_{\Omega_{\mathrm{D}}^{t_m}} \mathbf{curl}\, \boldsymbol{H}_h^m \cdot \boldsymbol{F}_h = \int_{\Omega_{\mathrm{S}}} \boldsymbol{J}_{\mathrm{S}}(t_m) \cdot \boldsymbol{F}_h \quad \forall \boldsymbol{F}_h \in \mathbf{curl}\left(\boldsymbol{\mathcal{N}}_h^{\Gamma}(\Omega_{\mathrm{D}}^{t_m})\right).$$

The following proposition shows that this problem is well posed.

Proposition 2. *There exists a unique solution to Problem 4, provided $\Delta t < \frac{2}{\overline{\sigma}\mu\|\boldsymbol{v}\|_\infty^2}$.*

Proof. To prove the well-posedness of the problem to be solved at each time step $m = 1, \ldots, M$, we resort to the classical theory of mixed problems (see [10], for instance) and prove the discrete *inf-sup* and the ellipticity in the discrete kernel conditions.

Since $\dim \boldsymbol{\mathcal{N}}_h^{\Gamma}(\Omega) < \infty$, for the former it is enough to prove that for each non-vanishing $\boldsymbol{F}_h \in \mathbf{curl}\left(\boldsymbol{\mathcal{N}}_h^{\Gamma}(\Omega_{\mathrm{D}}^{t_m})\right)$ there exists $\boldsymbol{G}_h \in \boldsymbol{\mathcal{N}}_h^{\Gamma}(\Omega)$ such that $\int_{\Omega_{\mathrm{D}}^{t_m}} \mathbf{curl}\, \boldsymbol{G}_h \cdot \boldsymbol{F}_h \neq 0$, which in turn follows immediately from the definition of the space $\boldsymbol{\mathcal{N}}_h^{\Gamma}(\Omega_{\mathrm{D}}^{t_m})$ by choosing $\boldsymbol{G}_h \in \boldsymbol{\mathcal{N}}_h^{\Gamma}(\Omega)$ such that $\boldsymbol{F}_h = \mathbf{curl}\, \boldsymbol{G}_h|_{\Omega_{\mathrm{D}}^{t_m}}$.

On the other hand, the ellipticity in the discrete kernel property means in this case that there exists $\alpha > 0$ such that

$$\frac{1}{\Delta t}\int_{\Omega}\mu\,|\boldsymbol{G}_h|^2+\int_{\Omega_{\rm C}^{t_m}}\frac{1}{\sigma}\,|\mathbf{curl}\,\boldsymbol{G}_h|^2-\int_{\Omega_{\rm C}^{t_m}}\boldsymbol{v}\times\mu\boldsymbol{G}_h\cdot\mathbf{curl}\,\boldsymbol{G}_h \\ \geq\alpha\,\|\boldsymbol{G}_h\|^2_{\mathrm{H}(\mathbf{curl};\Omega)}\qquad\forall\boldsymbol{G}_h\in\boldsymbol{\mathcal{K}}_h^m,$$

where the discrete kernel is

$$\boldsymbol{\mathcal{K}}_h^m:=\left\{\boldsymbol{G}_h\in\boldsymbol{\mathcal{N}}_h^\Gamma(\Omega):\ \int_{\Omega_{\rm D}^{t_m}}\mathbf{curl}\,\boldsymbol{G}_h\cdot\boldsymbol{F}_h=0\quad\forall\boldsymbol{F}_h\in\mathbf{curl}\left(\boldsymbol{\mathcal{N}}_h^\Gamma(\Omega_{\rm D}^{t_m})\right)\right\} \\ =\left\{\boldsymbol{G}_h\in\boldsymbol{\mathcal{N}}_h^\Gamma(\Omega):\ \mathbf{curl}\,\boldsymbol{G}_h=\mathbf{0}\text{ in }\Omega_{\rm D}^{t_m}\right\}.$$

To prove the ellipticity, we follow the same steps as in the proof of Theorem 1 that lead to (16) and obtain

$$\frac{1}{\Delta t}\int_{\Omega}\mu\,|\boldsymbol{G}_h|^2+\int_{\Omega_{\rm C}^{t_m}}\frac{1}{\sigma}\,|\mathbf{curl}\,\boldsymbol{G}_h|^2-\int_{\Omega_{\rm C}^{t_m}}\boldsymbol{v}\times\mu\boldsymbol{G}_h\cdot\mathbf{curl}\,\boldsymbol{G}_h \\ \geq\left(\frac{\mu}{\Delta t}-\frac{\gamma\mu\,\|\boldsymbol{v}\|_\infty}{2}\right)\|\boldsymbol{G}_h\|^2_{\mathrm{L}^2(\Omega)^3}+\left(\frac{1}{\overline{\sigma}}-\frac{\mu\,\|\boldsymbol{v}\|_\infty}{2\gamma}\right)\|\mathbf{curl}\,\boldsymbol{G}_h\|^2_{\mathrm{L}^2(\Omega_{\rm C}^{t_m})^3}$$

for all $\gamma>0$. Then, by taking $\gamma=\overline{\sigma}\mu\,\|\boldsymbol{v}\|_\infty$, we have that

$$\frac{1}{\Delta t}\int_{\Omega}\mu\,|\boldsymbol{G}_h|^2+\int_{\Omega_{\rm C}^{t_m}}\frac{1}{\sigma}\,|\mathbf{curl}\,\boldsymbol{G}_h|^2-\int_{\Omega_{\rm C}^{t_m}}\boldsymbol{v}\times\mu\boldsymbol{G}_h\cdot\mathbf{curl}\,\boldsymbol{G}_h \\ \geq\min\left\{\frac{\mu}{\Delta t}-\frac{\overline{\sigma}\mu^2\,\|\boldsymbol{v}\|^2_\infty}{2},\frac{1}{2\overline{\sigma}}\right\}\|\boldsymbol{G}_h\|^2_{\mathrm{H}(\mathbf{curl};\Omega)}$$

for all $\boldsymbol{G}_h\in\boldsymbol{\mathcal{K}}_h^m$. Hence, we conclude the ellipticity in the discrete kernel for any $\Delta t<\frac{2}{\overline{\sigma}\mu\|\boldsymbol{v}\|^2_\infty}$ with $\alpha=\min\left\{\frac{\mu}{\Delta t}-\frac{\overline{\sigma}\mu\|\boldsymbol{v}\|^2_\infty}{2},\frac{1}{2\overline{\sigma}}\right\}>0$. □

Problem 4 can be implemented by using a fixed mesh. However, in such a case, in general there will be tetrahedra which do not lie entirely in $\bar{\Omega}_{\rm C}^{t_m}$ or $\bar{\Omega}_{\rm D}^{t_m}$. To compute all but the first and last integrals from Problem 4 in these tetrahedra, we use a low-order quadrature rule with a large number of integration points. An additional difficulty of this implementation is that it is not simple to obtain a basis of the discrete space $\mathbf{curl}\left(\boldsymbol{\mathcal{N}}_h^\Gamma(\Omega_{\rm D}^{t_m})\right)$. Because of this, we have used the standard basis of $\boldsymbol{\mathcal{N}}_h^\Gamma(\Omega)$ to construct with their curls a (non-linearly independent) spanning set of that space. By so doing, at each time step we are led to solving a singular system of linear equations, well-determined in the sense that it has an (obviously non-unique) solution. This rank-degenerate linear system has to be solved in the least-square sense, what can be easily done in the MATLAB environment, for instance.

Let us come back now to the main goal of this section: to propose a well-posed discretization of Problem 3. We also use Nédélec edge elements from $\boldsymbol{\mathcal{N}}_h^\Gamma(\Omega)$, a backward Euler scheme on a uniform partition of $[0,T]$ and an approximate initial data $\boldsymbol{H}_{0h}\in\boldsymbol{\mathcal{N}}_h^\Gamma(\Omega)$ as for Problem 4. Thus we are led to the following scheme.

Problem 5. *Let* $\boldsymbol{H}^0_{h,\varepsilon} := \boldsymbol{H}_{0h}$. *For* $m = 1, \dots, M$, *find* $\boldsymbol{H}^m_{h,\varepsilon} \in \boldsymbol{\mathcal{N}}^\Gamma_h(\Omega)$ *such that*

$$\begin{aligned}\int_\Omega \mu \frac{\boldsymbol{H}^m_{h,\varepsilon} - \boldsymbol{H}^{m-1}_{h,\varepsilon}}{\Delta t} \cdot \boldsymbol{G}_h + \int_{\Omega_{\mathrm{C}}^{t_m}} \frac{1}{\sigma(t_m)} \operatorname{\mathbf{curl}} \boldsymbol{H}^m_{h,\varepsilon} \cdot \operatorname{\mathbf{curl}} \boldsymbol{G}_h \\ + \frac{1}{\varepsilon} \int_{\Omega_{\mathrm{D}}^{t_m}} \operatorname{\mathbf{curl}} \boldsymbol{H}^m_{h,\varepsilon} \cdot \operatorname{\mathbf{curl}} \boldsymbol{G}_h - \int_{\Omega_{\mathrm{C}}^{t_m}} \boldsymbol{v}(t_m) \times \mu \boldsymbol{H}^m_{h,\varepsilon} \cdot \operatorname{\mathbf{curl}} \boldsymbol{G}_h \\ = \frac{1}{\varepsilon} \int_{\Omega_{\mathrm{S}}} \boldsymbol{J}_{\mathrm{S}}(t_m) \cdot \operatorname{\mathbf{curl}} \boldsymbol{G}_h \qquad \forall \boldsymbol{G}_h \in \boldsymbol{\mathcal{N}}^\Gamma_h(\Omega).\end{aligned}$$

The following lemma shows that the above problem is also well posed.

Proposition 3. *For all* $\varepsilon \in (0, \underline{\sigma})$ *and* $\Delta t < \frac{2}{\overline{\sigma}\mu\|\boldsymbol{v}\|^2_\infty}$, *there exists a unique solution to Problem 5.*

Proof. The Lax-Milgram Lemma ensures the existence and uniqueness of solution of the problem to be solved at each time step $m = 1, \dots, M$. Indeed, by repeating the steps from the proof of Proposition 2, we obtain

$$\begin{aligned}\frac{1}{\Delta t} \int_\Omega \mu \left|\boldsymbol{G}_h\right|^2 + \int_{\Omega_{\mathrm{C}}^{t_m}} \frac{1}{\sigma} \left|\operatorname{\mathbf{curl}} \boldsymbol{G}_h\right|^2 + \frac{1}{\varepsilon} \int_{\Omega_{\mathrm{D}}^{t_m}} \left|\operatorname{\mathbf{curl}} \boldsymbol{G}_h\right|^2 - \int_{\Omega_{\mathrm{C}}^{t_m}} \boldsymbol{v} \times \mu \boldsymbol{G}_h \cdot \operatorname{\mathbf{curl}} \boldsymbol{G}_h \\ \geq \min\left\{ \frac{\mu}{\Delta t} - \frac{\overline{\sigma}\mu^2 \left\|\boldsymbol{v}\right\|^2_\infty}{2}, \frac{1}{2\overline{\sigma}} \right\} \left\|\boldsymbol{G}_h\right\|^2_{\mathrm{H}(\mathbf{curl};\Omega_{\mathrm{C}}^{t_m})} \\ + \frac{1}{\underline{\sigma}} \left\|\boldsymbol{G}_h\right\|^2_{\mathrm{H}(\mathbf{curl};\Omega_{\mathrm{D}}^{t_m})} \qquad \forall \boldsymbol{G}_h \in \boldsymbol{\mathcal{N}}^\Gamma_h(\Omega).\end{aligned}$$

Thus, the ellipticity follows for any $\Delta t < \frac{2}{\overline{\sigma}\mu\|\boldsymbol{v}\|^2_\infty}$ with $\alpha = \min\left\{ \frac{\mu}{\Delta t} - \frac{\overline{\sigma}\mu^2\|\boldsymbol{v}\|^2_\infty}{2}, \frac{1}{2\overline{\sigma}} \right\} > 0$. □

Let us remark that the same mesh is used over the whole time interval. The motion of the workpiece affects the domains of all but the first and the last integrals of Problem 5. To compute integrals on those tetrahedra that do not lie entirely in one of the domains, $\Omega_{\mathrm{C}}^{t_m}$ or $\Omega_{\mathrm{D}}^{t_m}$, we also use a low-order quadrature rule with a large number of integration points. The implementation of Problem 5 is very simple. It does not need moving meshes and the number of unknowns is kept reasonably small (it equals the number of inner edges of the mesh). However, the analysis of convergence of this penalized formulation as all the parameters, ε, h and Δt, go to zero remains an open problem.

3. Numerical results

In this section, we will report some numerical results obtained with a MATLAB code which implements the penalization technique described above. First, it is applied to solve a test problem with a known analytical solution, in order to illustrate the convergence of the method with respect to the penalization and the discretization parameters. Next, we consider a problem with cylindrical symmetry, which will allow us to compare the results with those obtained with another code based on an axisymmetric formulation introduced and analyzed in [3, 4].

3.1. Test 1: Problem with a known analytical solution. We approximate the solution of the following source problem:

$$\begin{aligned}\operatorname{\mathbf{curl}} \boldsymbol{H} &= \sigma \boldsymbol{E} + \sigma\, \boldsymbol{v} \times \mu \boldsymbol{H} \qquad \text{in } (0,T) \times \Omega, \\ \partial_t(\mu \boldsymbol{H}) + \operatorname{\mathbf{curl}} \boldsymbol{E} &= \boldsymbol{f} \qquad \text{in } (0,T) \times \Omega,\end{aligned}$$

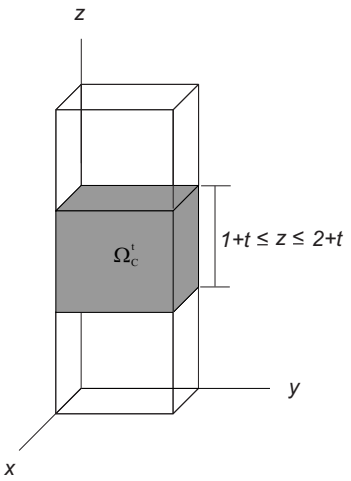

FIGURE 2. Test 1. Sketch of the domain.

where $\boldsymbol{f}$ is a given data defined in the whole domain $\Omega := (0,1)\times(0,1)\times(0,3)$ and $T = \frac{1}{2}$.

We assume that the initial position of the workpiece is the cube $(0,1)\times(0,1)\times(1,2)$ and that it moves as a rigid body with velocity $\boldsymbol{v} = \boldsymbol{e}_z$, so that $\Omega_{\mathrm{C}}^t = (0,1)\times(0,1)\times(1+t,2+t)$ (see Figure 2).

We have used for this test $\mu = \mu_0 = 4\pi\times10^{-7}\,\mathrm{Hm}^{-1}$, $\sigma = 10^6\,(\Omega\mathrm{m})^{-1}$ in Ω_{C}^t and $\sigma = 0$ in Ω_{D}^t. Notice that we can freely choose any Δt in the time interval $[0,T]$, because it satisfies the restriction $\Delta t < \frac{2}{\overline{\sigma}\mu\|\boldsymbol{v}\|_\infty^2} = 1.5915$ given in Proposition 3. The data $\boldsymbol{f}$ has been chosen so that the analytical solution be

$$\boldsymbol{H}(t,\boldsymbol{x}) := t^2\begin{pmatrix}\varphi(t,z)\\ \varphi(t,z)\\ z\end{pmatrix}$$

with

$$\varphi(t,z) := \begin{cases} (z-1-t)^2\,(z-2-t)^2\,, & z\in[1+t,2+t],\\ 0 & z\notin[1+t,2+t],\end{cases}$$

and

$$\boldsymbol{E}(t,\boldsymbol{x}) := \begin{cases} \frac{1}{\sigma(t)}\,\mathbf{curl}\,\boldsymbol{H}(t,\boldsymbol{x}) - \boldsymbol{v}(t,\boldsymbol{x})\times\mu\boldsymbol{H}(t,\boldsymbol{x}) & \text{in } \Omega_{\mathrm{C}}^t,\\ 0 & \text{in } \Omega_{\mathrm{D}}^t.\end{cases}$$

Notice that $\mathbf{curl}\,\boldsymbol{H}(t) = \boldsymbol{0}$ in Ω_{D}^t for all $t\in[0,T]$. This is the constraint that will be penalized, since there is no source current $\boldsymbol{J}_{\mathrm{S}}$ in this test. Given $\varepsilon > 0$, the corresponding penalized problem reads as follows: find $\boldsymbol{H}_\varepsilon \in \mathrm{L}^2(0,T;\mathrm{H}(\mathbf{curl};\Omega))\cap$

$\mathrm{H}^1(0,T;\mathrm{H}(\mathbf{curl};\Omega)')$ such that

$$\begin{aligned}
&\frac{d}{dt}\int_\Omega \mu \boldsymbol{H}_\varepsilon\cdot\boldsymbol{G}+\int_{\Omega_{\mathrm{C}}^t}\frac{1}{\sigma}\,\mathbf{curl}\,\boldsymbol{H}_\varepsilon\cdot\mathbf{curl}\,\boldsymbol{G}\\
&-\int_{\Omega_{\mathrm{C}}^t}\boldsymbol{v}\times\mu\boldsymbol{H}_\varepsilon\cdot\mathbf{curl}\,\boldsymbol{G}+\frac{1}{\varepsilon}\int_{\Omega_{\mathrm{D}}^t}\mathbf{curl}\,\boldsymbol{H}_\varepsilon\cdot\mathbf{curl}\,\boldsymbol{G}\\
&=\int_\Omega \boldsymbol{f}\cdot\boldsymbol{G}+\int_\Gamma \boldsymbol{g}\cdot\boldsymbol{G}\qquad\forall\boldsymbol{G}\in\mathrm{H}(\mathbf{curl};\Omega),\\
&\boldsymbol{H}_\varepsilon(0)=\boldsymbol{H}_0\qquad\text{in }\Omega,
\end{aligned}$$

where the exact values of $\boldsymbol{f}$ in Ω and $\boldsymbol{g}:=\boldsymbol{E}\times\boldsymbol{n}$ on Γ have been used as problem data.

These equations have been discretized by using Nédélec finite elements in space and the backward Euler method in time, leading to a scheme similar to that in Problem 5. To compute the integrals on those tetrahedra that do not lie entirely in Ω_{C}^t or Ω_{D}^t, we have used a simple average of the discontinuous integrand in 2925 equispaced points of the tetrahedron. We have also solved the problem with larger numbers of integration points to check that the reported results are essentially indifferent to this number.

The error of the computed solution depends on the penalization parameter ε, the mesh size h and the time-step Δt. First, we focused on analyzing the dependence on ε. With this in view, we have also solved the corresponding mixed formulation of this problem, which reads as follows: find $\boldsymbol{H}\in\mathrm{L}^2(0,T;\mathrm{H}(\mathbf{curl};\Omega))\cap\mathrm{H}^1(0,T;\mathrm{H}(\mathbf{curl};\Omega)')$ and $\boldsymbol{E}\in\mathrm{L}^2(0,T;\mathrm{H}(\mathrm{div}^0;\Omega_{\mathrm{D}}^t))$ such that

$$\begin{aligned}
&\frac{d}{dt}\int_\Omega \mu \boldsymbol{H}\cdot\boldsymbol{G}+\int_{\Omega_{\mathrm{C}}^t}\frac{1}{\sigma}\,\mathbf{curl}\,\boldsymbol{H}\cdot\mathbf{curl}\,\boldsymbol{G}\\
&-\int_{\Omega_{\mathrm{C}}^t}\boldsymbol{v}\times\mu\boldsymbol{H}\cdot\mathbf{curl}\,\boldsymbol{G}+\int_{\Omega_{\mathrm{D}}^t}\mathbf{curl}\,\boldsymbol{G}\cdot\boldsymbol{E}\\
&=\int_\Omega \boldsymbol{f}\cdot\boldsymbol{G}+\int_\Gamma \boldsymbol{g}\cdot\boldsymbol{G}\qquad\forall\boldsymbol{G}\in\mathrm{H}(\mathbf{curl};\Omega),\\
&\int_{\Omega_{\mathrm{D}}^t}\mathbf{curl}\,\boldsymbol{H}\cdot\boldsymbol{F}=0\qquad\forall\boldsymbol{F}\in\mathrm{H}(\mathrm{div}^0;\Omega_{\mathrm{D}}^t),\\
&\boldsymbol{H}(0)=\boldsymbol{H}_0\qquad\text{in }\Omega.
\end{aligned}$$

To assess the dependence of the errors on the penalization parameter ε, we have solved both problems with the same fixed mesh and time-step and with varying ε. In such a case, the difference between the solutions $\boldsymbol{H}_{h,\varepsilon}^k$ and $\boldsymbol{H}_h^k$ of these two problems is due only to the penalization. We have computed the following percentage errors:

$$100\,\frac{\max\limits_{1\le k\le M}\left\|\boldsymbol{H}_{h,\varepsilon}^k-\boldsymbol{H}_h^k\right\|_{\mathrm{L}^2(\Omega)^3}}{\max\limits_{1\le k\le M}\left\|\boldsymbol{H}_h^k\right\|_{\mathrm{L}^2(\Omega)^3}}$$

and

$$100\,\frac{\sqrt{\Delta t}\left\{\sum_{k=1}^M\left\|\boldsymbol{H}_{h,\varepsilon}^k-\boldsymbol{H}_h^k\right\|_{\mathrm{H}(\mathbf{curl};\Omega)}^2\right\}^{1/2}}{\sqrt{\Delta t}\left\{\sum_{k=1}^M\left\|\boldsymbol{H}_h^k\right\|_{\mathrm{H}(\mathbf{curl};\Omega)}^2\right\}^{1/2}},$$

which are time-discrete forms of the errors in $\mathrm{L}^\infty(0,T;\mathrm{L}^2(\Omega)^3)$ and $\mathrm{L}^2(0,T;\mathrm{H}(\mathbf{curl};\Omega))$ norms, respectively.

TABLE 1. Test 1. Percentage penalization errors.

ε	ε/σ	$\mathrm{L}^\infty(0,T;\mathrm{L}^2(\Omega)^3)$	$\mathrm{L}^2(0,T;\mathrm{H}(\mathbf{curl};\Omega))$
10^2	10^{-4}	0.008162	0.102870
10^1	10^{-5}	0.001187	0.015876
10^0	10^{-6}	0.000125	0.001680
10^{-1}	10^{-7}	0.000015	0.000169

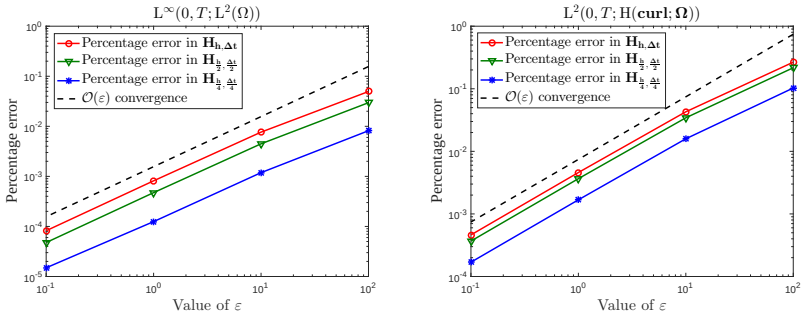

FIGURE 3. Test 1. Percentage penalization error curves in $\mathrm{L}^\infty(0,T;\mathrm{L}^2(\Omega)^3)$ (left) and $\mathrm{L}^2(0,T;\mathrm{H}(\mathbf{curl};\Omega))$ (right) norms for several discretizations. The coarsest one corresponds to a mesh with 144 elements and a time-step $\Delta t = \frac{1}{20}$.

We report in Table 1 the penalization errors on a fixed mesh with 9216 elements and with a time-step $\Delta t = \frac{1}{80}$ (i.e., $M = 40$), for different values of the penalization parameter ε. We also include in the table the relative values of ε with respect to the conductivity $\sigma = 10^6$ used in this test.

The numerical results from Table 1 show clearly a linear convergence with respect to the parameter ε. The penalization errors are actually very small, even for not so small relative values of the penalization parameter; however, for values of $\varepsilon/\sigma < 10^{-7}$, the linear convergence deteriorates mildly due to ill-conditioning of the resulting linear system.

The results do not change significantly when the experiments are repeated with different time-steps and mesh-sizes. This can be clearly seen in Figure 3, where penalization error curves in the same norms as above are shown for different combinations of time-steps and mesh-sizes. Indeed, all the curves show a clear linear dependence of the error with respect to the penalization parameter.

Next, in order to assess the dependence of the errors on the discretization parameters h and Δt, we have chosen a sufficiently small fixed value of the penalization parameter: $\varepsilon = 10^{-1}$. As can be seen from Table 1, for such a small value of ε, the penalization errors are absolutely negligible. For this test, we have computed the actual errors, namely the differences between the obtained numerical solution and the analytical one. We report in Tables 2 and 3 the percentage errors for $\boldsymbol{H}$ in time-discrete $\mathrm{L}^\infty(0,T;\mathrm{L}^2(\Omega)^3)$ and $\mathrm{L}^2(0,T;\mathrm{H}(\mathbf{curl};\Omega))$ norms, respectively.

In order to appreciate simultaneously the dependence of the errors on h and Δt, we have plotted in Figure 4 the errors that appear within boxes in Tables 2 and 3 versus the number of degrees of freedom (d.o.f.). These values within boxes correspond to the errors of the present method when using different discretization parameters h and Δt with time-steps Δt proportional to the mesh-sizes h. In these

TABLE 2. Test 1. Percentage errors for $\boldsymbol{H}$ in $\mathrm{L}^\infty(0,T;\mathrm{L}^2(\Omega)^3)$ norm ($\varepsilon = 10^{-1}$) for several discretizations. The coarsest one corresponds to a mesh with 144 elements and a time-step $\Delta t = \frac{1}{20}$.

	h	$h/2$	$h/3$	$h/4$	$h/5$
Δt	12.880	9.561	8.805	8.532	8.400
$\Delta t/2$	10.827	6.502	5.328	4.854	4.617
$\Delta t/3$	10.377	5.723	4.345	3.745	3.431
$\Delta t/4$	10.215	5.421	3.937	3.262	2.897
$\Delta t/5$	10.138	5.275	3.733	3.012	2.610

TABLE 3. Test 1. Percentage errors for $\boldsymbol{H}$ in $\mathrm{L}^2(0,T;\mathrm{H}(\mathbf{curl};\Omega))$ norm ($\varepsilon = 10^{-1}$) for several discretizations. The coarsest one corresponds to a mesh with 144 elements and a time-step $\Delta t = \frac{1}{20}$.

	h	$h/2$	$h/3$	$h/4$	$h/5$
Δt	15.512	11.458	10.470	10.169	9.996
$\Delta t/2$	13.319	8.209	6.727	6.172	5.908
$\Delta t/3$	12.773	7.200	5.509	4.767	4.355
$\Delta t/4$	12.565	6.798	4.975	4.133	3.682
$\Delta t/5$	12.463	6.615	4.712	3.806	3.303

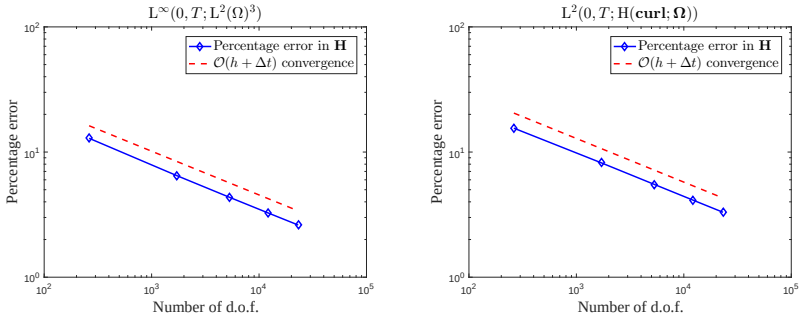

FIGURE 4. Test 1. Percentage discretization error curves in $\mathrm{L}^\infty(0,T;\mathrm{L}^2(\Omega)^3)$ (left) and $\mathrm{L}^2(0,T;\mathrm{H}(\mathbf{curl};\Omega))$ (right) norms ($\varepsilon = 10^{-1}$).

figures, d.o.f. refers to the number of unknowns of the system to be solved at each time step (which is roughly speaking proportional to h^{-3}). A clear linear dependence $\mathcal{O}(h+\Delta t)$ can be easily observed from these curves.

3.2. Test 2. A problem with cylindrical symmetry and rigid motion. Comparison with an axisymmetric code. We consider the cylindrically symmetric geometry sketched in Figure 5. As we advanced in the introduction, our method is a first step to solve magneto-mechanical models and our present goal is to validate the genuine electromagnetic model by considering Ω_{C}^t as a data. In

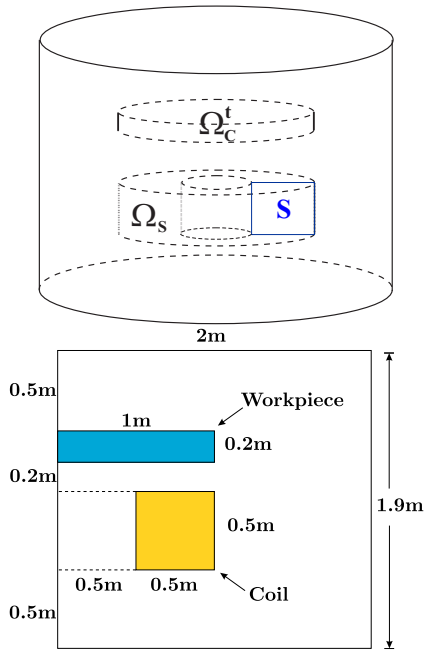

FIGURE 5. Test 2. Sketch of the domain (up). Meridian section (down).

this case we will assume that the workpiece is not deformed but it changes its position over the time; more precisely, it moves as a rigid body with velocity equal to $\boldsymbol{v} = 50\boldsymbol{e}_z$ (length is written in meters and time in seconds).

The source current density supported in Ω_S is given by

$$\boldsymbol{J}_S(t,\boldsymbol{x}) = \frac{I(t)}{\text{area}(S)}\boldsymbol{e}_\theta \quad \text{in } \Omega_S, \qquad \text{with} \quad \boldsymbol{e}_\theta := \frac{1}{\sqrt{x^2+y^2}}\begin{pmatrix} -y \\ x \\ 0 \end{pmatrix}$$

being the azimuthal unit vector in cylindrical coordinates and $I(t)$ the source current intensity. In this test, we have proceeded as in [15] and used a damped sinusoidal function $I(t) := I_0 \exp(-\beta t)\sin(\omega t)$ with $I_0 = 3.07\times 10^5$ A, $\beta = 5327\,\text{s}^{-1}$ and $\omega = 34.315\,\text{s}^{-1}$ (see Figure 6). Concerning the physical parameters, we have taken $\mu = \mu_0 = 4\pi \times 10^{-7}\,\text{Hm}^{-1}$, $\sigma = 10^4\,(\Omega\text{m})^{-1}$ in the workpiece and $T = 0.002\,\text{s}$. We notice that also in this case we can freely choose any Δt in the time interval $[0, 0.002]$, because restriction $\Delta t < \frac{2}{\overline{\sigma}\mu\|\boldsymbol{v}\|_\infty^2} = 0.0637$ is widely satisfied.

In this case, there is no analytical solution available. However, since the source current density field has only azimuthal non-zero component and the workpiece moves only vertically, it is known that the solution has cylindrical symmetry. Such an axisymmetric problem with moving domains has been studied in [3, 4], where a two-dimensional scalar formulation written in terms of the azimuthal component of a magnetic vector potential has been proposed. Under appropriate assumptions, a piecewise linear discretization of this formulation was proved to converge with optimal order error estimates in terms of h and Δt. We have used a code of this method on a very fine mesh and with a very small time-step, to build a reference solution of the problem.

Figure 7 shows the two dimensional fine mesh of the meridian section that we have used for the axisymmetric code. Concerning the 3D meshes, we have exploited

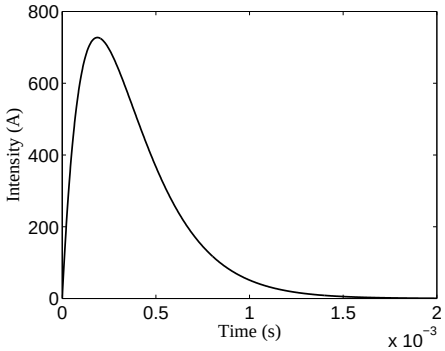

FIGURE 6. Test 2. Source current intensity (A) vs. time (s).

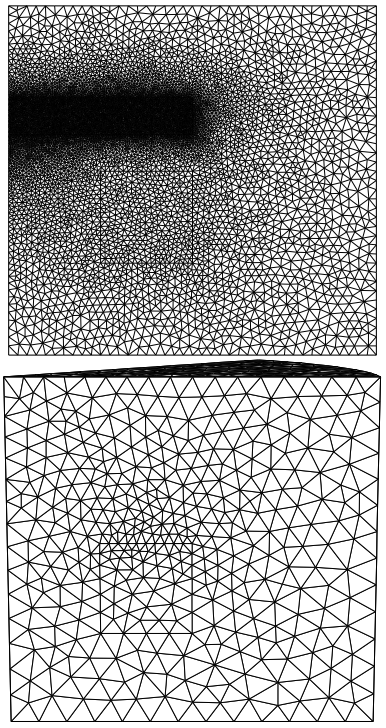

FIGURE 7. Test 2. Mesh used for the axisymmetric code (up). Coarsest mesh used for the 3D code (down).

the symmetry of the problem and solved it in 1/8 of the whole domain to reduce the number of degrees of freedom. We show in Figure 7, the coarsest used mesh.

As in the previous subsection, we have solved the problem with the penalization parameter $\varepsilon = 10^{-1}$. We have used several 3D meshes with mesh-sizes and time-steps conveniently reduced, namely the time-steps have been chosen roughly speaking proportional to the respective mesh-sizes. We report in Table 4 the data of each of the used meshes.

TABLE 4. Test 2. Total numbers of degrees of freedom (d.o.f.) and time steps (M) for each of the used meshes.

Mesh	$\mathcal{T}_h^1$	$\mathcal{T}_h^2$	$\mathcal{T}_h^3$	$\mathcal{T}_h^4$	$\mathcal{T}_h^5$
d.o.f.	20,616	36,097	61,987	120,750	238,861
M	40	48	58	72	90

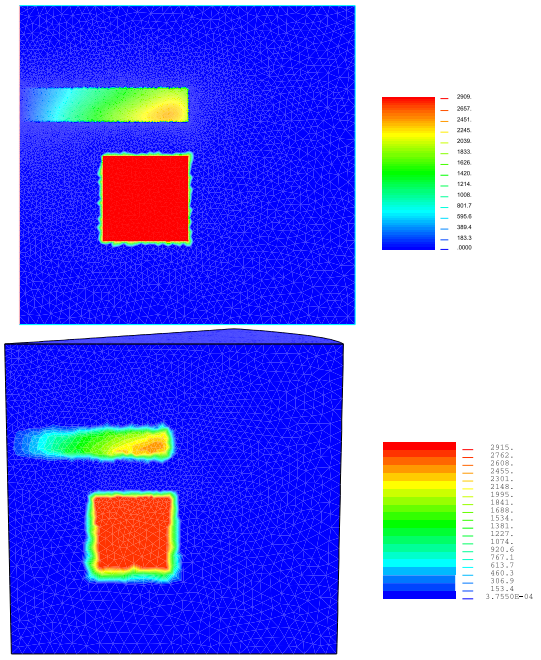

FIGURE 8. Test 2. Modulus of the current density at time 0.00018 s computed with the axisymmetric code (up) and the 3D code on $\mathcal{T}_h^5$ with $\varepsilon = 10^{-1}$ (down).

In the applications, the quantity of most practical interest is typically the current density, $\boldsymbol{J} := \mathbf{curl}\, \boldsymbol{H}$, induced in the workpiece Ω_{C}^t. Figure 8 shows the modulus of $\boldsymbol{J}$ obtained with the axisymmetric and the 3D codes at the time in which the input current intensity attains its maximum ($t = 0.00018\,\mathrm{s}$). For the 3D code, we have used the finest mesh $\mathcal{T}_h^5$. A very good agreement between the results obtained with these two methods can be clearly appreciated. To illustrate the comparison for a non-local quantity over the time, we report in Figure 9 the induced current intensity in the meridian section ($\theta = 0$) of Ω_{C}^t which will be denoted by Θ; i.e. the quantity plotted is $\int_\Theta \boldsymbol{J} \cdot \boldsymbol{e}_\theta \, \mathrm{d}S$). This quantity is computed with the 3D code on the different meshes over the time and also with the axisymmetric code.

For a more quantitative assessment, we report in Figure 10 the $\mathrm{L}^2(\Omega_{\mathrm{C}}^t)^3$ norm of the errors of the current densities computed with the 3D code on the different meshes over the time. To allow for comparison, we also include in this figure the $\mathrm{L}^2(\Omega_{\mathrm{C}}^t)^3$ norm of the current density obtained from the reference solution. As can be seen from this figure, the errors of the computed current density are very large for the coarsest 3D meshes, but they reduce appropriately as the mesh-size and the time-step become smaller.

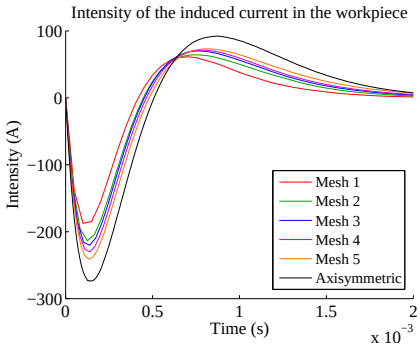

FIGURE 9. Test 2. Current intensity (A) induced in the worpiece vs. time (s) on meshes $\mathcal{T}_h^i$, $i = 1, \ldots, 5$, and with the reference solution.

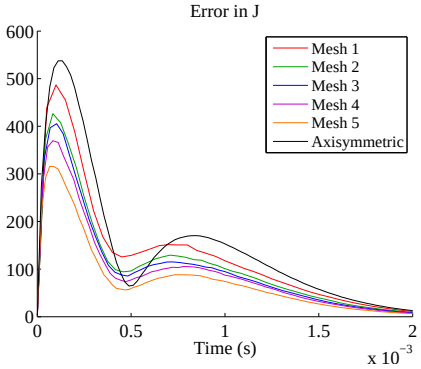

FIGURE 10. Test 2. $\mathrm{L}^2(\Omega_{\mathrm{C}}^t)^3$ norm of the errors of the current densities computed with the 3D code on meshes $\mathcal{T}_h^i$, $i = 1, \ldots, 5$, over the time. $\mathrm{L}^2(\Omega_{\mathrm{C}}^t)^3$ norm of the current density obtained from the reference solution is also plotted.

In physical applications with motion, such us EMF or magnetic levitation, the induced current density is used to compute the Lorentz force density, $\boldsymbol{F} := \boldsymbol{J} \times \boldsymbol{B}$, that acts on the workpiece. Figure 11 shows the vertical resultant of this force, $\int_{\Omega_{\mathrm{C}}^t} \boldsymbol{J} \times \boldsymbol{B} \cdot \boldsymbol{e}_z$, computed with the 3D code on the different meshes over the time, as well as the same quantity resulting from the reference solution.

It can be seen from Figure 11 that the vertical resultant of the Lorentz force computed with the 3D code provides a very good approximation of the same quantity computed with the reference solution, even for the coarsest meshes. Moreover, as the mesh-size and the time-step become smaller, the approximation clearly improves.

Finally, Figure 12 shows the value of the Lorentz force density versus the radial coordinate in the workpiece at a fixed time. With this aim, we have fixed the azimuthal and vertical coordinates and chosen the time at which the maximum value of this density force is reached. Notice that, as expected, the largest values of this density force in the workpiece are attained just above the coil.

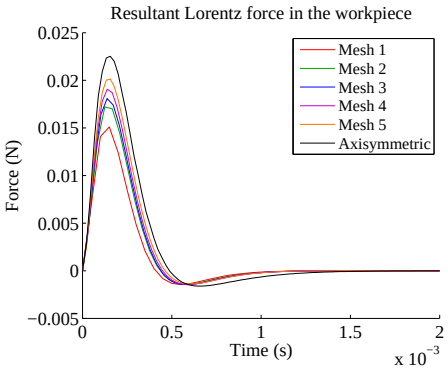

FIGURE 11. Test 2. Vertical resultant of the Lorentz force computed with the 3D code on meshes $\mathcal{T}_h^i$, $i = 1, \ldots, 5$, and with the reference solution over the time.

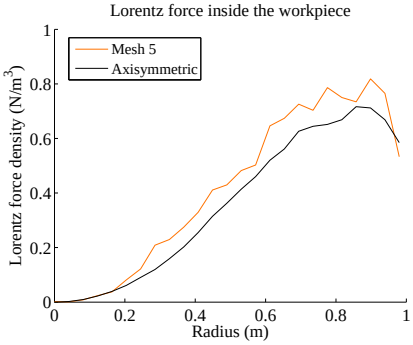

FIGURE 12. Test 2. Lorentz force density ($\mathrm{N/m^3}$) vs. radial coordinate (m) in the workpiece; vertical coordinate $z = 1.2578$ m and time $t = 1.55 \times 10^{-4}$ s.

4. Conclusions

We have introduced a numerical method based on a magnetic field formulation to approximate the transient eddy current problem in the presence of moving non magnetic conductors. We have proposed a numerical technique where the only unknown is the magnetic field in the whole domain, which allows us to use a fixed mesh over the time. The proposal is based on replacing the dielectric by a fake conductor with a very low electrical conductivity to impose the curl-free constraint in the dielectric domain. This so-called penalty strategy leads to a parabolic problem with discontinuous coefficients; to compute the corresponding integrals in those elements that do not lie entirely in the dielectric or the conducting domains, we have used low-order quadrature rules with a large number of integration points. The methodology is suitable to model conductors which move freely in a dielectric medium, even in the case that the convective terms arising from this motion could be non-negligible in Ohm's law.

We have reported numerical results for two different test problems, which demonstrate that the choice of the fake conductivity in the dielectric is not critical at all; indeed, choosing this conductivity five or six orders of magnitude below that of the

conducting parts leads to results indistinguishable from those obtained with a more expensive mixed method in which the curl-free constraint is explicitly imposed. On the other hand, extremely low values of the fake conductivity should be avoided since they could lead to ill-conditioned matrices. We have also reported numerical results for a problem with cylindrical symmetry and rigid motion. The comparison of the results with those arising from an axisymmetric model are highly promissory.

From the theoretical point of view, further exploration on this subject is challenging, since the uniqueness of solution of the continuous model and convergence results for the proposed numerical scheme remain to be proved.

Acknowledgments

All the authors were partially supported by FEDER/Ministerio de Ciencia, Innovación y Universidades–Agencia Estatal de Investigación under the research project MTM2017-86459-R. First and fourth authors were partially supported by FEDER and Xunta de Galicia under research project GRC2013/014 and GRC GI-1563 ED431C 2017/60. Second author was partially supported by Universidad Nacional de Colombia through the call for mobility Hermes 6632. Third author was partially supported by CONICYT-Chile through the project AFB170001 of the PIA Program: Concurso Apoyo a Centros Científicos y Tecnológicos de Excelencia con Financiamiento Basal.

References

[1] Alonso-Rodríguez, A., Hiptmair, R. and Valli, A. Mixed finite element approximation of eddy current problems. *IMA Journal of Numerical Analysis*, 24 (2004), pp. 255–271.

[2] Alonso A. and Valli, A., *Eddy Current Approximation of Maxwell Equations: Theory, Algorithms and Applications*. Springer–Verlag, Italia (2010).

[3] Bermúdez, A., Muñoz, R., Reales, C., Rodríguez, R. and Salgado, P. A transient eddy current problem on a moving domain. Mathematical analysis. *SIAM Journal on Mathematical Analysis*, 45 (2013), pp. 3629–3650.

[4] Bermúdez, A., Muñoz, R., Reales, C., Rodríguez, R. and Salgado, P. A transient eddy current problem on a moving domain. Numerical analysis. *Advances in Computational Mathematics*, 42 (2016), pp. 757–789.

[5] Bouillault, F., Buffa, A., Maday, Y. and Rapetti, F. Simulation of a magneto-mechanical damping machine: analysis, discretization, results. *Computer Methods in Applied Mechanics and Engineering*, 23-24 (2002), pp. 2587–2610.

[6] Buffa, A., Maday, Y. and Rapetti, F. Applications of the mortar element method to 3D electromagnetic moving structures. In *Computational Electromagnetics*. Lecture Notes in Computational Science and Engineering, 28 (2003), pp. 35–50.

[7] Buffa, A., Maday, Y. and Rapetti, F. A sliding mesh-mortar method for a two dimensional eddy currents model of electric engines. *M2AN. Mathematical Modelling and Numerical Analysis*, 35 (2001), pp. 191–228.

[8] El-Azab, A., Garnich, M. and Kapoor, A. Modeling of the electromagnetic forming of sheet metals: state-of-art an future needs. *Journal of Materials Processing Technology*, 142 (2003), pp. 744–754.

[9] Gaier, C. and Haas, H. Edge element analysis of magnetostatic and transient eddy current fields using $\overrightarrow{H}$ formulations. *IEEE Transactions on Magnetics*, 31 (1995), pp. 1460–1463.

[10] Girault, V. and Raviart, P.A. *Finite Element Methods for Navier-Stokes Equations. Theory and Algorithms.* New York: Springer-Verlag, 1986.

[11] Qiu, L., Xiao, Y., Deng, C., LiZ., Xu, Y., Li, Z. and Chang, P. Electromagnetic-structural analysis and improved loose coupling method in electromagnetic forming process. *International Journal of Advanced Manufacturing Technology*, 89 (2017), pp. 701-710.

[12] Meddahi, S. and Selgas, V. An H-based FEM-BEM formulation for a time dependent eddy current problem. *Applied Numerical Mathematics*, 58 (2008), pp. 1061–1083.

[13] Showalter R. E. Degenerate evolution equations and applications. *Indiana University Mathematics Journal*, 23 (1974), pp. 655–677.

[14] Showalter R. E. *Monotone Operators in Banach Space and Nonlinear Partial Differential Equations*. American Mathematical Society Publications, Providence, 1997.
[15] Siddiqui, M. A., Correia, J. P. M., Ahzi1, S. and Belouettar, S., A numerical model to simulate electromagnetic sheet metal forming. *International Journal of Material Forming*, 1, Suppl. (2008), pp. 1387–1390.
[16] Ženíšek, A. *Nonlinear Elliptic and Evolution Problems and their Finite Element Approximations*. London: Academic Press, 1990.

Departamento de Matemática Aplicada, Universidade de Santiago de Compostela, 15706, Santiago de Compostela, Spain
E-mail: alfredo.bermudez@usc.es, mpilar.salgado@usc.es

Escuela de Matemáticas, Universidad Nacional de Colombia, Sede Medellín, Colombia
E-mail: blopezr@unal.edu.co

CI^2MA, Departamento de Ingeniería Matemática, Universidad de Concepción, Casilla 160-C, Concepción, Chile
E-mail: rodolfo@ing-mat.udec.cl